Polymer 96 (2016) 63–69

Contents lists available at ScienceDirect

Polymer

journal homepage: www.elsevier.com/locate/polymer

Selective dispersion of single-walled carbon nanotubes by binaphthyl-based conjugated polymers: Integrated experimental and simulation approach

Sa Hoon Min [a], Hye-In Kim [d], Kyung-su Kim [c], Inhwan Cha [c], Seonggyun Ha [c], Wan Soo Yun [c], Sang Kyu Kwak [a], Jong-Ho Kim [d], Byeong-Su Kim [a, b, **], Changsik Song [c, *]

[a] Department of Energy Engineering, School of Energy and Chemical Engineering, Ulsan National Institute of Science and Technology (UNIST), 50 UNIST-gil, Ulsan, 44919, Republic of Korea
[b] Department of Chemistry, School of Natural Science, Ulsan National Institute of Science and Technology (UNIST), 50 UNIST-gil, Ulsan, 44919, Republic of Korea
[c] Department of Chemistry, Sungkyunkwan University (SKKU), Suwon, 440-746, Republic of Korea
[d] Department of Chemical Engineering, Hanyang University, Ansan, 426-791, Republic of Korea

ARTICLE INFO

Article history:
Received 23 February 2016
Received in revised form
22 April 2016
Accepted 26 April 2016
Available online 27 April 2016

Keywords:
Single-walled carbon nanotubes
Conjugated polymers
Dispersion
Binaphthyl
Selectivity
MD simulation

ABSTRACT

Hybrids of π-conjugated polymers and single-walled carbon nanotubes (SWNTs) are an intriguing class of materials owing to their interesting electric and optoelectronic properties. Herein, we synthesized three types of 1,1′-binaphthyl-incorporated conjugated polymers with thiophene bridges. It was found that the molecular structure of the π-conjugated polymers affected the selective dispersion of individual SWNT species: the hexyl-substituted PBHT preferred (8,7) SWNT while polymers with no alkyl groups on the thiophenes (PBT and PB2T) preferred (8,6) species. Molecular dynamics (MD) simulations also revealed that the polymers were able to wrap around SWNTs and showed selective interactions with the SWNT species.

1. Introduction

Hybrid materials of single-walled carbon nanotubes (SWNTs) and π-conjugated polymers have attracted great attention since the combination of each component's benefits is expected to afford synergistic effects [1–3]. Due to their excellent electric, optoelectronic, and mechanical properties, SWNTs have been used in sensors, actuators, and optoelectronic devices [4–6]. SWNTs have also been applied to the enhancement of polymer's material properties, such as mechanical strength and conductivity. π-Conjugated polymers also have interesting electronic/optoelectronic properties that stem from conjugation of π-electrons. The combination of SWNTs and π-conjugated polymers is expected to offer both enhanced electronic properties, such as charge-carrier mobility, and interesting electronic couplings between them.

Several π-conjugated polymers are known to well disperse SWNTs due to favorable interactions between the SWNT sidewalls and the π-conjugated backbones of the polymers [7–12]. Interestingly, depending on the structures of the polymer main chain, molecular weights, and substitution patterns, π-conjugated polymers enable the selective dispersion of carbon nanotubes. For example, Nicholas and co-workers reported that poly(9,9-dioctylfluorene) (PFO) can selectively disperse semiconducting SWNTs, especially those with smaller diameters [13]. Bao and co-workers utilized regio-regular poly(3-alkylthiophene)s and investigated the effect of alkyl chains, solvent and temperatures for selective sorting of semiconducting SWNTs [14]. Other π-conjugated polymers, such as poly(phenylene-ethynylnene) (PPE), polycarbazole, and polyazomethines, have been reported for selective dispersion of SWNTs [9,15,16].

* Corresponding author.
** Corresponding author. Department of Chemistry, School of Natural Science, Ulsan National Institute of Science and Technology (UNIST), 50 UNIST-gil, Ulsan, 44919, Republic of Korea.
E-mail addresses: bskim19@unist.ac.kr (B.-S. Kim), songcs@skku.edu (C. Song).

http://dx.doi.org/10.1016/j.polymer.2016.04.063
0032-3861/

Binaphthyl-containing conjugated polymers are an interesting class of materials since they deploy optically active 1,1′-binaphthyl units, the property arising from the restricted rotation around the 1,1′-biaryl bond. Specifically, 1,1′-binaphthyl is a privileged structure that has been extensively used in chiral recognition and catalysis [17–19]. When binaphthyls are incorporated into polythiophene backbones, interesting electronic properties have been observed such as chiral analyte sensing or dihedral angle-dependent electroactivities [20,21]. Recently, Nakashima and co-workers reported the use of binaphthyl-containing PFOs for the separation of right- and left-handed SWNTs [22]. In addition, Therien and co-workers investigated the single-handed helical wrapping of SWNTs by controlling the dihedral angle of binaphthyl components in PPE-based conjugated polymers [23]. However, no example of binaphthyl-incorporated polythiophene derivatives for selective dispersion of SWNTs has been reported so far.

Herein, we report the synthesis of 1,1′-binaphthyl-incorporated π-conjugated polymers and their use in the selective dispersion of SWNTs. UV–vis–NIR absorption spectra and photoluminescence-excitation (PLE) profiles reveal that the backbone structure of π-conjugated polymers plays an important role in determining the selectivity of SWNT dispersion. We also conducted molecular dynamics (MD) simulations which supported the observations that the selective interactions between 1,1′-binaphthyl-incorporated conjugated polymers and SWNT sidewalls depend on the polymer structures.

2. Experiment

2.1. Materials and characterization

All the chemicals were purchased from Sigma–Aldrich, TCI, Alfa Aesar, Samchun Chemical and used without further purification. SWNTs were purchased from Sigma Aldrich (compound number: 724777, 0.7–1.4 nm diameter, ≥80.0% carbon as SWNT composition). Typical Williamson ether synthesis from 6,6′-dibromo-1,1′-binaphthalene-2,2′-diol furnished 6,6′-dibromo-2,2′-didecyloxy-1,1′-binaphthalene (**1**) [24]. 2,5-Bis(trimethylstannyl)thiophene (**3**) [25] and 5,5′-bis(trimethylstannyl)-2,2′-bithiophene (**4**) [26] were prepared according to the literature. ^{1}H and ^{13}C NMR spectra were recorded on a Bruker 500 MHz spectrometer. The chemical shifts are reported in ppm (δ) with TMS as an internal standard and the coupling constants (J) are expressed in Hz. Ultraviolet–visible-Near IR (UV–vis–NIR) absorption data were acquired on a UV-2600 (Shimadzu, Japan) spectrophotometer and UV–vis spectra on a UV-1800 (Shimadzu, Japan). SWNT dispersion underwent with a tip sonicator (VCX-130, Sonics & Materials. Inc, USA). NIR fluorescence was collected by a fluorescence spectrophotometer (Nano Logs, HORIBA, USA) equipped with an InGaAs detector. The average molecular weight and polydispersity index (PDI) of the polymers were determined on a gel permeation chromatograph (GPC) by using THF as eluent and polystyrene as a standard on an Agilent Technologies 1260 Infinity. Liquid-chromatograph mass spectra (LC-MS) were obtained on Agilent Technologies 1260 Infinity and quadruple mass 6130 model.

2.2. Synthesis of 2,2′-(2,2′-bis(decyloxy)-[1,1′-binaphthalene]-6,6′-diyl)bis(4,4,5,5-tetramethyl -1,3,2-dioxaborolane) (2)

A mixture with 6,6′-dibromo-2,2′-bis(decyloxy)-1,1′-binaphthalene (**1**) (43 mg, 0.060 mmol), bis(pinacolato)diboron (34 mg, 0.13 mmol), Pd(dppf)Cl_2 (5.0 mg, 8 mol%), and potassium acetate (35 mg 0.35 mmol) in 1.0 mL DMSO was stirred at 80 °C for 6 h under a nitrogen atmosphere. The reaction mixture was cooled to room temperature, poured into 10 mL of ice water, filtrated, and then purified by column chromatography on a silica gel with ethyl acetate/hexane (1/20 vol/vol) as an eluent to afford a yellow powder (27 mg, 54%). ^{1}H NMR ($CDCl_3$, 500 MHz): δ 8.38 (s, 2H), 7.96 (d, J = 8.5 Hz, 2H), 7.52 (dd, J_a = 8.5 Hz, J_b = 1.0 Hz, 2H), 7.38 (d, J = 9.0 Hz, 2H), 7.09 (d, J = 8.5 Hz, 2H), 3.96–3.86 (m, 4H), 1.35 (s, 24H), 1.28–1.19 (m, 32H) 0.87 (t, J = 7.0 Hz, 6H); ^{13}C NMR ($CDCl_3$, 125 MHz): δ 155.6, 136.4, 136.0, 130.6, 130.0, 128.6, 124.6, 120.3, 115.5, 83.7, 69.6, 31.9, 29.7, 29.5, 29.5, 29.4, 29.4, 29.3, 29.2, 25.6, 24.9, 24.9, 22.7, 14.1. MS (HRMS): m/z calculated for $C_{52}H_{76}B_2O_6Na$: 840.7 [M + Na^+]; found: 841.4 [M + Na^+].

2.3. Synthesis of poly[{6,6′-dibromo-2,2′-bis(decyloxy)-1,1′-binaphthalene}-alt-{2,5-bis(trimethylstannyl)thiophene}] (PBT)

6,6′-dibromo-2,2′-bis(decyloxy)-1,1′-binaphthalene (**1**) (44 mg, 0.061 mmol), 2,5-bis(trimethylstannyl)thiophene (**3**) (24.9 mg, 0.061 mmol), and tetrakis(triphenylphosphine) palladium(0) (3.5 mg, 5 mol%) were added to a flame-dried 10 mL Schlenk flask under nitrogen. Dry DMF (1.0 mL) was then added via a syringe and the reaction mixture was purged with nitrogen for 10 min. The reaction mixture was then heated to 120 °C for polymerization. After 24 h, the partially soluble solid was precipitated by addition of 30 mL methanol, washed through a Soxhlet extraction with methanol for 48 h to remove oligomer or residual catalyst and then with chloroform for 24 h to obtain the chloroform-soluble polymer solution. The resulting solution was concentrated and dried under vacuum to obtain polymer **PBT** as a yellow solid (67% yield). GPC (polystyrene standard): M_n = 12,600, M_w = 22,900, PDI = 1.81.

2.4. Synthesis of poly[{6,6′-dibromo-2,2′-bis(decyloxy)-1,1′-binaphthalene}-alt-{5,5′-bis(trimethylstannyl)-2,2′-bithiophene}] (PB2T)

PB2T was prepared according to the literature [1]. GPC (polystyrene standard): M_n = 17,300, M_w = 34,800, PDI = 2.01.

2.5. Synthesis of poly[2,2′-(2,2′-bis(decyloxy)-[1,1′-binaphthalene]-6,6′-diyl) bis(4,4,5,5-tetramethyl-1,3,2-dioxaborolane)-alt-2,5-dibromo-3-hexylthiophene] (PBHT)

2,2′-(2,2′-bis(decyloxy)-[1,1′-binaphthalene]-6,6′-diyl)bis(4,4,5,5-tetramethyl-1,3,2-dioxaborolane) (**2**) (28 mg, 0.034 mmol), 2,5-dibromo-3-hexylthiophene (**5**) (11 mg, 0.034 mmol), and tetrakis-(triphenylphosphine) palladium(0) (2.0 mg, 5 mol%) were added to a flame-dried 10 mL Schlenk flask under nitrogen. Dry DMF (1.0 mL) was then added via a syringe and the reaction mixture was purged and stirred under nitrogen for 30 min, and then 0.3 mL aqueous solution with sodium carbonate (22 mg, 0.20 mmol) was gradually added by a dropping funnel. The reaction mixture was heated to 80 °C and stirred for 24 h. After being cooled to room temperature, the partially soluble solid was precipitated by addition of 30 mL methanol, washed through a Soxhlet extraction with methanol for 48 h to remove oligomer or residual catalyst and then with chloroform for 24 h to obtain the chloroform-soluble polymer solution. The solution was concentrated and dried under vacuum to obtain **PBHT** as a yellow solid (75% yield). GPC (polystyrene standard): M_n = 4,500, M_w = 6,500, PDI = 1.45.

2.6. General procedure for dispersion of SWNTs with polymers in NMP

A 1.0 mg portion of SWNTs was added into 1 mL of *N*-methylpyrrolidone (NMP) in which a 1.0 mg portion of a desired polymer was dissolved. The resulting mixture was then sonicated for 1 h in an ice bath with a probe tip sonicator (8–10 Watts). After

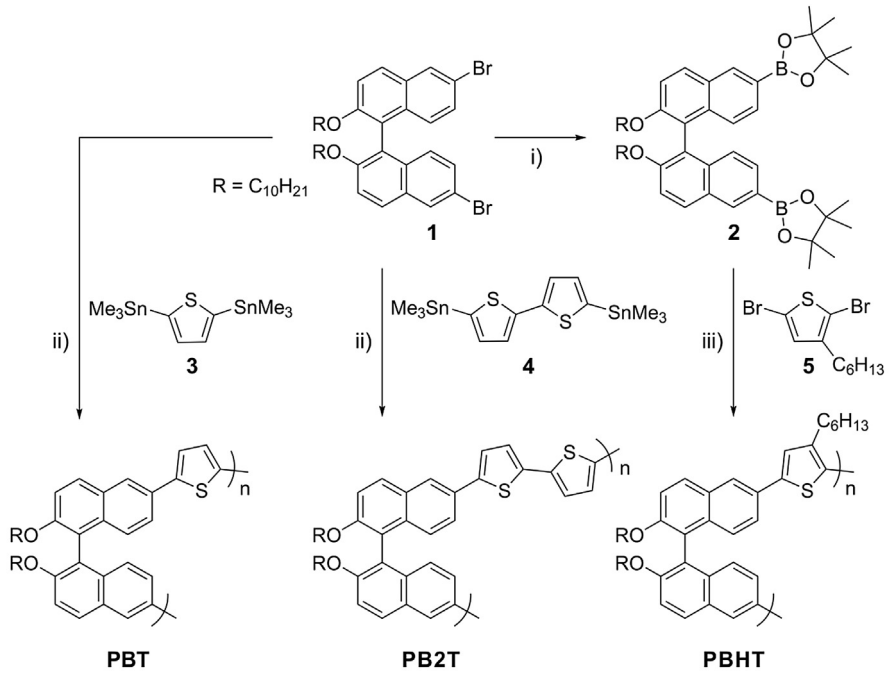

[a]Reagents and conditions: i) B_2pin_2 (2.2 eq), KOAc (5.8 eq), $Pd(dppf)Cl_2$ (8 mol%) DMSO, 80 °C, 6 h, 54%. ii) $Pd(PPh_3)_4$ (5 mol%), DMF, 100 °C, overnight, 67%. iii) $Pd(PPh_3)_4$ (5 mol%), Na_2CO_3 (6 eq), H_2O, DMF, 80 °C, 24 h, 75%.

Scheme 1. Structure and Synthetic Scheme of 1,1′-Binaphthyl-Incorporated Conjugated Polymers PBT, PBHT, and PB2T[a].

centrifugation of the solution at 12,200 *g* for 30 min, the supernatant was obtained to get a SWNT/polymer dispersion.

2.7. NIR fluorescence measurement and photoluminescence-excitation mapping of SWNT/polymer dispersions

The NIR fluorescence of the SWNT/polymer dispersions was measured by excitation at 740 nm using a Xenon lamp with exposure for 10 s at room temperature. The SWNT/polymer dispersions underwent PL-mapping by changing the excitation wavelengths from 560 to 760 nm with exposure for 10 s at room temperature.

2.8. Simulation details

To simulate the selective interaction between binaphthyl-containing conjugated polymers (**PBT** and **PBHT**) and SWNTs with different chiralities, all-atom models were constructed by using AMBER forcefield. The generalized AMBER forcefield (GAFF) [27] and the AMBER 99 forcefield [28] parameters were used for the conjugated polymers and SWNTs, respectively. All atomic partial charges on the conjugated polymers were calculated by AM1-BCC method in AmberTools14 [29], and the partial charges of the SWNT were set to zero. Infinitely long SWNTs with the chirality numbers of (8,6) and (8,7) were modeled by TubeGen 3.4 [30] and were placed in the center of each rectangular simulation box with periodic boundary condition. In the initial conformation, a single **PBT** or **PBHT** chain comprised of 4 monomer units was wrapped around each SWNT which was in close contact with the binaphthyl and thiophene group of the conjugated polymers. The simulation box was filled with about 1000 NMP molecules parameterized by GAFF forcefield. Each topology was converted to GROMACS-compatible format by ACPYPE script [31] for initial input file.

The MD simulations were performed using GROMACS 5.1.1 package [32] with a time step of 1.0 fs. After energy minimization step of initial condition, the systems were heated up to 300 K over 100-ps canonical (NVT) ensemble and 500-ps isothermal-isobaric (NPT) ensemble. Long MD simulations for the production run were then calculated at 300 K and 1 bar with NPT ensemble by using the V-rescale thermostat with a coupling constant of 0.1 ps and Parrinello–Rahman barostat with a coupling constant of 2.0 ps. The pressure coupling was not applied along the axis of the SWNT. The cutoff distance for the short-range van der Waals and electrostatic interactions was set to 1.0 nm, and the particle mesh Ewald (PME) method was applied to the long-range electrostatic interactions. All bond length related to hydrogen atoms were constrained with the LINCS algorithm [33]. Visualization in this work was performed using VMD package [34].

3. Results and discussion

1,1′-Binaphthyl-incorporated conjugated polymers with thiophenes were prepared via palladium-catalyzed cross coupling polymerizations between binaphthyl- and thiophene-derivatives (Scheme 1). We set out the synthesis with bromination, followed by alkylation, of commercially available 1,1′-bi-2,2′-naphthol to provide dibromobinaphthyl **1**. The long decyl group ensures the solubility of the resulting polymers. Stille cross-coupling condensation of dibromobinaphthyl **1** with bis(trimethylstannyl)-thiophene (**3**) and -bithiophene (**4**) furnished 1,1′-binaphthyl-incorporated conjugated polymers **PBT** and **PB2T**, respectively [20]. In order to examine the effect of substituents on the thiophene moiety, we attempted to synthesize hexyl-substituted polymer **PBHT** in a similar manner. However, the preparation of bis(stannyl)thiophene with a hexyl group was not successful due to the steric hindrance between the 2- and 3-positions of the thiophene. Instead, we

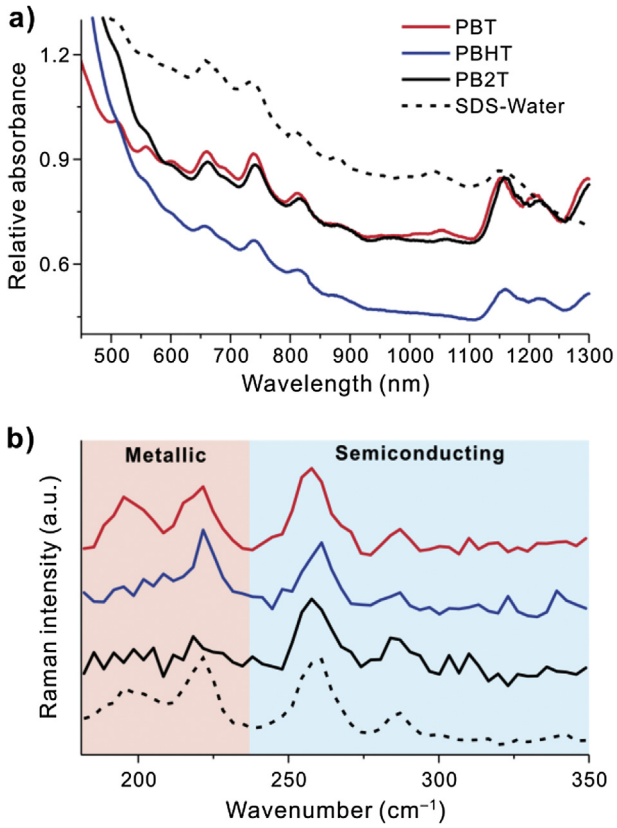

Fig. 1. (a) UV–vis–NIR absorption spectra of dispersed SWNTs with PBT (red), PBHT (blue), and PB2T (black, 1/4 dilution) in NMP solutions. The dotted black line is dispersed SWNTs with 1% sodium dodecyl sulfate (SDS) in water for comparison. (b) The radial breathing mode (RBM) of Raman spectra (excitation at 633 nm) of dispersed SWNTs as in (a). (For interpretation of the references to color in this figure legend, the reader is referred to the web version of this article.)

introduced pinacol-boronate groups at the 6,6′-positions of the binaphthyl via Pd-catalyzed C–B bond formation. Suzuki–Miyaura cross-coupling condensation of bis(pinacol-boronate) **2** with dibromo-3-hexylthiophene **5** produced the desired polymer **PBHT**. ^{1}H-NMR spectroscopy results of all polymers were well matched with the intended structures. Gel permeation chromatography with polystyrene standards in THF suggested that number-average molecular weights (M_n) of **PBT**, **PB2T**, and **PBHT** are 12.6 k, 17.3 k, and 4.5 k, respectively, with a polydispersity index of 1.45–2.10. Further experimental details for the synthesis are available in the Supporting Information.

Optical absorbance studies revealed that 1,1′-binaphthyl-incorporated conjugated polymers are effective in the dispersion of SWNTs. Fig. 1 shows the UV–vis–NIR absorption spectra of SWNTs dispersed in *N*-methyl-2-pyrrolidone (NMP) solutions of three 1,1′-binaphthyl polymers (1 mg/mL). We set out the dispersion with 0.7–1.4 nm-diameter, CoMoCAT® SWNTs in which both metallic and semiconducting SWNTs were present. Considering diameter of the SWNTs, the absorption spectra are dominated by the E_{11} (>900 nm) and E_{22} (500–600 nm in wavelength) bands of the semiconducting SWNTs [35]. Due to the onset of the absorption of the 1,1′-binaphthyl conjugated polymers (~500 nm, see Supporting Information), the E_{22} band of metallic SWNTs was not clearly observed. As shown in Fig. 1, all three 1,1′-binaphthyl conjugated polymers (**PBT**, **PB2T**, and **PBHT**) appears to disperse SWNTs well in NMP. However, the relative amounts of SWNTs solubilized by polymers were affected by the polymer structures; for example, **PB2T**, which has two thiophene units, was able to disperse approximately four times more SWNTs than **PBT**, which has only one thiophene unit, as judged by optical densities (Fig. 1). We attributed this difference to the increased conjugation length of **PB2T**. With more thiophene units are attached, the resulting larger conjugation backbones can interact strongly with SWNTs. Interestingly, when an alkyl group was attached to the thiophene, the quantity of the SWNTs dispersed in the solvent appeared to decrease; **PBHT** afforded less dispersion of SWNTs than did **PBT**. The decreased ability of SWNT dispersion by alkylation is not clear yet. We postulate that alkylation may slightly distort the conjugation planes between thiophene and naphthalene units. However, other factors that may play a role such as molecular weights of polymers and chirality of 1,1′-binaphthyls. Raman spectra were also measured for SWNTs dispersed with binaphthyl polymers (Fig. 1b). The radial breathing mode (RBM) frequencies of the Raman spectra are inversely proportional to the diameter of carbon nanotubes [36]. The RBM region is shown in Fig. 1b obtained using an excitation wavelength of 633 nm. When compared to SWNTs dispersed with 1% SDS in water, the binaphthyl polymers seem to disperse semiconducting nanotubes in a similar fashion. We observed slight differences in the intensities of metallic species according to polymers, but they are not so clear and need further investigation. Although it is premature to draw definite conclusions regarding molecular structures, the 1,1′-binaphthyl-incorporated conjugated polymers with thiophene units were effective in dispersing of SWNTs at least in an organic solvent.

PLE mapping of SWNT solutions with 1,1′-binaphthyl conjugated polymers revealed that the slight change of the molecular structures may result in selective dispersion of SWNT species. The UV–vis–NIR spectra show all of the solubilized SWNTs species, regardless of their state of bundling. In contrast, the photoluminescence spectra show only sufficiently-debundled or isolated SWNT species. As shown in Fig. 2, PLE mappings were conducted on three SWNT/1,1′-binaphthyl conjugated polymer systems. We tried to disperse SWNTs in pure NMP not containing any polymers. However, the stability of SWNT dispersion was very limited in the pure NMP, showing no measurable PL. The conjugated polymers with one and two thiophenes, **PBT** and **PB2T**, respectively, resulted in very similar PLE mapping patterns, although **PB2T** was able to disperse SWNTs more in UV–vis–NIR (Fig. 1). In the PLE maps, several SWNTs species were mainly observed: (7,6), (9,4), (9,5), (8,6), (8,7), and (11,4). Among them, fluorescence intensities from (8,6) and (8,7) were most evident. We have normalized the PL intensity of the SWNTs dispersed on the basis of the quantum yield (QY) of each chirality (Table S1). Then, we have calculated the intensity ratios between (8,6) and (8,7) SWNTs. According to the previous literature [37], the QYs were found to be 0.624 (6.25×10^{-5} electron/photon) and 0.92 (6.25×10^{-5} electron/photon) for (8,6) and (8,7) SWNTs, respectively. The normalized intensity ratio (r) of (8,6)/(8,7) was very similar for **PBT** ($r = 1.7$) and **PB2T** ($r = 1.6$); (8,6) species were dispersed more with these polymers. Intriguing results were found in the case of alkyl-substituted polymer **PBHT** ($r = 1.3$). Even though the kinds of SWNT species were more or less similar, **PBHT** resulted in more dispersion of (8,7) than that of (8,6), which is opposite to the case of **PBT** and **PB2T**. Interestingly, the slight alteration of molecular structure resulted in the reverse of the preference in SWNT dispersion. It is not easy to predict intuitively what kind of molecular interactions cause this difference since (8,6) and (8,7) SWNTs are very similar in size and electronic structures.

MD simulation has been widely explored to suggest the specific interaction and structure of various macromolecules onto SWNTs [22,38–40]. Thus, we conducted atomistic MD simulations to investigate the interaction of 1,1′-binaphthyl-incorporated

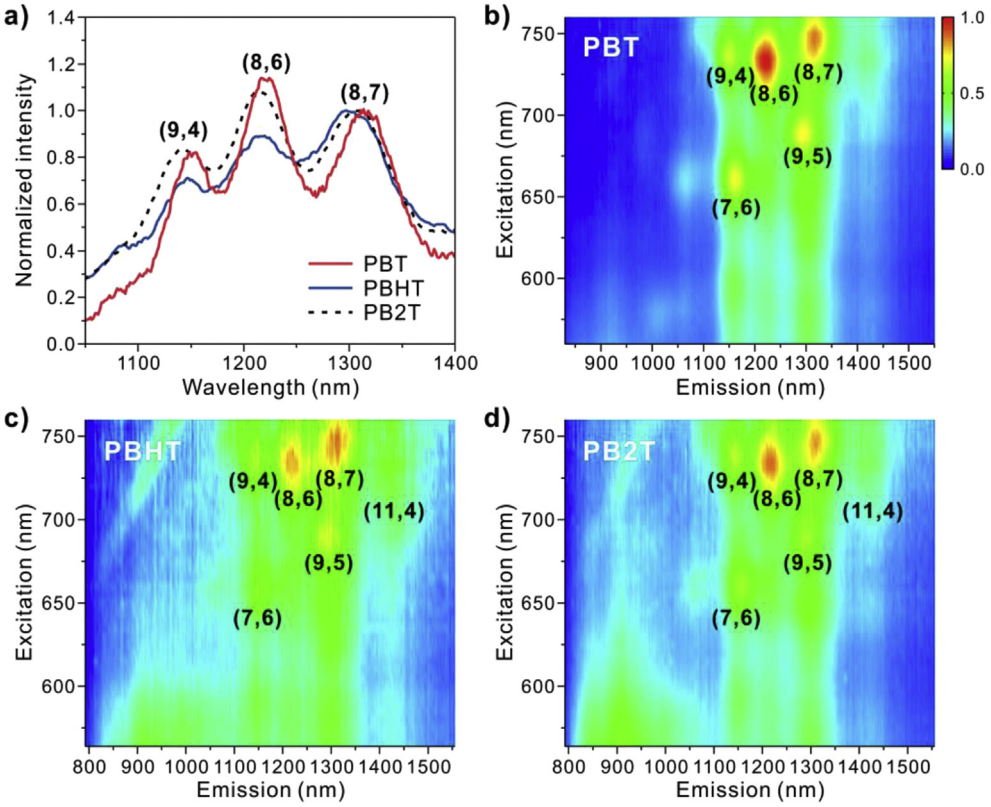

Fig. 2. (a) Fluorescence spectra of SWNT/polymer dispersion in NMP. Photoluminescence-excitation (PLE) mapping of dispersed SWNTs with **PBT** (b), **PBHT** (c), and **PB2T** (d) in NMP. The labels represent the identified SWNT species.

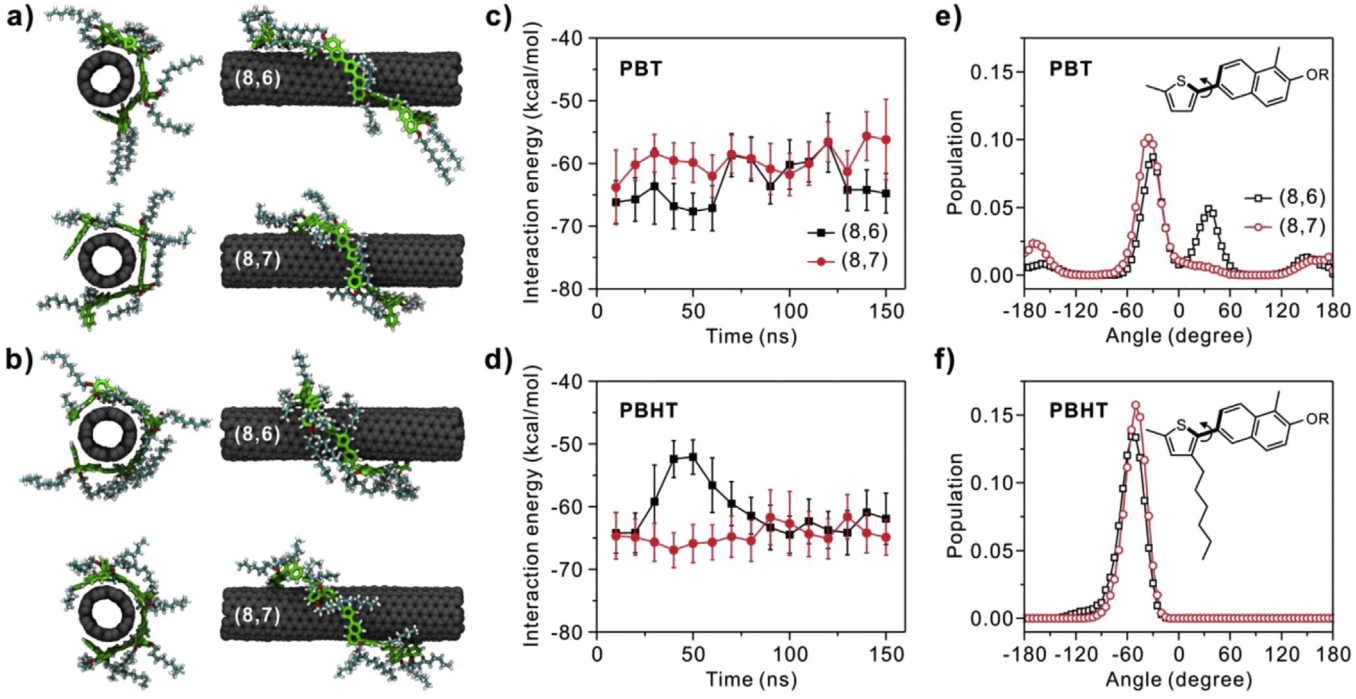

Fig. 3. Snapshots of (a) **PBT** and (b) **PBHT** conformations onto (8,6) and (8,7) SWNT after 150 ns MD simulation at 300 K. Binaphthyl and thiophene groups are shown with green, and NMP solvent molecules are not shown for clarity. Pairwise interaction energies of binaphthyl and thiophene group in (c) **PBT** and (d) **PBHT** toward SWNTs. Population analysis of dihedral angle between binaphthyl group and thiophene group in (e) **PBT** and (f) **PBHT** from the last 50-ns trajectories. (For interpretation of the references to color in this figure legend, the reader is referred to the web version of this article.)

conjugated polymers (**PBT** and **PBHT**) toward SWNTs having different chirality modes, by using AMBER forcefield [41,42]. In the initial conformation, binaphthyl and thiophene groups of the conjugated polymers were in close contact with the surface of SWNTs, in order to induce an efficient wrapping phenomenon of the conjugated polymer during the MD simulations. From the 150-ns MD simulation, as shown in Fig. 3a,b, it is observed that both **PBT** and **PBHT** were well wrapped around (8,6) and (8,7) SWNTs, which were in agreement with the experimental results.

The pairwise interaction energy can provide useful information for the specific interactions between the conjugated polymers and SWNTs. To understand the π–π interactions between the conjugated polymers and SWNTs, we focused on the binaphthyl and thiophene group in the conjugated polymer. Thus, the interaction energy was calculated as follows:

$$E_{interaction} = E_{complex} - \left(E_{poly} + E_{SWNT}\right)$$

where E_{poly}, E_{SWNT}, and $E_{complex}$ are the potential energy of the binaphthyl and thiophene group in the conjugated polymer, SWNT, and their complex, respectively.

Fig. 3c,d shows the interaction energy of SWNT/**PBT** and SWNT/**PBHT** in their complex, respectively. The relatively high absolute value of the initial interaction energies gradually converged through the MD simulation, representing the equilibrium state of the wrapping process of **PBT** and **PBHT** around each SWNT. The last 50-ns averaged interaction energy of (8,6) SWNT/**PBT** is −61.9 kcal/mol, which is higher than that of (8,7) SWNT/**PBT** (−57.9 kcal/mol). On the other hand, **PBHT** has a slightly strong interaction with (8,7) SWNT with an average interaction energy of −64.1 kcal/mol, compared with (8,6) SWNT (−62.6 kcal/mol). Thus, it supports the fact that the selective dispersion of SWNTs is achieved by 1,1′-binaphthyl-incorporated conjugated polymers, depending on the polymer structure.

The main difference between **PBT** and **PBHT** is the introduction of hexyl chains into the thiophene group. This hexyl group can lead to the steric hindrance in the dihedral torsional motion between thiophene group and its adjacent binaphthyl group. Indeed, the population analysis indicates a distinct difference in the dihedral angle distribution between **PBT** and **PBHT**, as shown in Fig. 3e,f. In the last 50-ns trajectories, the dihedral angle between thiophene and binaphthyl group in **PBT** represents a nearly planar conformation with strong peaks at about −30° or 30°. However, in the case of **PBHT**, the dominant dihedral angle between thiophene and binaphthyl group near the hexyl chain increases in comparison with that in **PBT,** with a peak at −50°. It implies that the hexyl group influences the equilibrium conformation of thiophene and binaphthyl group onto SWNTs. Consequently, it suggests that the structural difference in the 1,1′-binaphthyl-incorporated conjugated polymers may account for the selective interactions to SWNTs.

4. Conclusions

In conclusion, we synthesized 1,1′-binaphthyl-incorporated conjugated polymers with thiophene bridges (**PBT**, **PB2T**, and **PBHT**) for the dispersion of single-walled carbon nanotubes (SWNTs). UV–vis–NIR spectroscopy revealed that π–π interaction between the polymer backbone and SWNT sidewalls plays an important role in SWNT dispersion. **PB2T**, which has two thiophene bridges, was able to disperse SWNT most effectively, while **PBHT**, with a hexyl group attached at the thiophene, dispersed the least amount of SWNTs among them. Photoluminescence-excitation (PLE) mapping showed the individually dispersed SWNT species and there was a slight preference for (8,6) over (8,7) in the case of **PBT** and **PB2T**. Interestingly, however, the hexyl-substituted **PBHT** showed the reversed preference; more (8,7) was dispersed than (8,6). This unexpected result of a variation in preference according to subtle differences in the molecular structure was supported by the MD simulations. In the simulation, the 1,1′-binaphthyl-incorporated conjugated polymers were able to wrap around the SWNTs. In accord with the experimental result, **PBT** showed a stronger interaction toward (8,6) than toward (8,7), while the hexyl-substituted **PBHT** showed the a slightly more stable interaction with (8,7) over (8,6).

Acknowledgment

This study was supported by Civil-Military Technology Cooperation Program of Korea funded by the Ministry of Trade, Industry and Energy. This work was also supported by the Basic Science Research Program through the National Research Foundation of Korea (NRF) funded by the Ministry of Science, ICT and Future Planning (NRF-2014R1A2A1A11051877, 2015R1A2A2A04003160 and 2010-0028684). The author thanks the Nano Material Development Program through the National Research Foundation of Korea (NRF) funded by the Ministry of Education, Science and Technology (MEST), Republic of Korea (2012M3A7B4049644). B.K. and S.K. acknowledge the computation resources from UNIST-HPC and KISTI (KSC-2016-C2-0003).

Appendix A. Supplementary data

Supplementary data related to this article can be found at http://dx.doi.org/10.1016/j.polymer.2016.04.063.

References

[1] E. Kymakis, G.A.J. Amaratunga, Single-wall carbon nanotube/conjugated polymer photovoltaic devices, Appl. Phys. Lett. 80 (2002) 112–114.
[2] S.D. Stranks, J.K. Sprafke, H.L. Anderson, R.J. Nicholas, Electronic and mechanical modification of single-walled carbon nanotubes by binding to porphyrin oligomers, ACS Nano 5 (2011) 2307–2315.
[3] C. Bounioux, P. Díaz-Chao, M. Campoy-Quiles, M.S. Martín-González, A.R. Goñi, R. Yerushalmi-Rozen, C. Müller, Thermoelectric composites of poly(3-hexylthiophene) and carbon nanotubes with a large power factor, Energy Environ. Sci. 6 (2013) 918–925.
[4] Rajesh, T. Ahuja, D. Kumar, Recent progress in the development of nano-structured conducting polymers/nanocomposites for sensor applications, Sens. Actuators, B 136 (2009) 275–286.
[5] F. Wang, H. Gu, T.M. Swager, Carbon nanotube/polythiophene chemiresistive sensors for chemical warfare agents, J. Am. Chem. Soc. 130 (2008) 5392–5393.
[6] C. Wei, L. Dai, A. Roy, T.B. Tolle, Multifunctional chemical vapor sensors of aligned carbon nanotube and polymer composites, J. Am. Chem. Soc. 128 (2006) 1412–1413.
[7] Y.-L. Zhao, J.F. Stoddart, Noncovalent functionalization of single-walled carbon nanotubes, Acc. Chem. Res. 42 (2009) 1161–1171.
[8] N. Berton, F. Lemasson, J. Tittmann, N. Stürzl, F. Hennrich, M.M. Kappes, M. Mayor, Copolymer-controlled diameter-selective dispersion of semiconducting single-walled carbon nanotubes, Chem. Mater 23 (2011) 2237–2249.
[9] H. Ozawa, T. Fujigaya, S. Song, H. Suh, N. Nakashima, Different chiral selective recognition/extraction of (n, m)single-walled carbon nanotubes using copolymers carrying a carbazole or fluorene moiety, Chem. Lett. 40 (2011) 470–472.
[10] F.A. Lemasson, T. Strunk, P. Gerstel, F. Hennrich, S. Lebedkin, C. Barner-Kowollik, W. Wenzel, M.M. Kappes, M. Mayor, Selective dispersion of single-walled carbon nanotubes with specific chiral indices by poly(N-decyl-2,7-carbazole), J. Am. Chem. Soc. 133 (2011) 652–655.
[11] M. Tange, T. Okazaki, S. Iijima, Selective extraction of large-diameter single-wall carbon nanotubes with specific chiral indices by poly(9,9-dioctylfluorene-alt-benzothiadiazole), J. Am. Chem. Soc. 133 (2011) 11908–11911.
[12] P. Gerstel, S. Klumpp, F. Hennrich, A. Poschlad, V. Meded, E. Blasco, W. Wenzel, M.M. Kappes, C. Barner-Kowollik, Highly selective dispersion of single-walled carbon nanotubes via polymer wrapping: a combinatorial study via modular conjugation, ACS Macro Lett. 3 (2014) 10–15.
[13] A. Nish, J.-Y. Hwang, J. Doig, R.J. Nicholas, Highly selective dispersion of single-

walled carbon nanotubes using aromatic polymers, Nat. Nanotechnol. 2 (2007) 640–646.
[14] H.W. Lee, Y. Yoon, S. Park, J.H. Oh, S. Hong, L.S. Liyanage, H. Wang, S. Morishita, N. Patil, Y.J. Park, et al., Selective dispersion of high purity semiconducting single-walled carbon nanotubes with regioregular poly(3-alkylthiophene)s, Nat. Commun. 2 (2011) 541.
[15] W. Gomulya, V. Derenskyi, E. Kozma, M. Pasini, M.A. Loi, Polyazines and polyazomethines with didodecylthiophene units for selective dispersion of semiconducting single-walled carbon nanotubes, Adv. Funct. Mater 25 (2015) 5858–5864.
[16] C.D. Von Bargen, C.M. MacDermaid, O.-S. Lee, P. Deria, M.J. Therien, J.G. Saven, Origins of the helical wrapping of phenyleneethynylene polymers about single-walled carbon nanotubes, J. Phys. Chem. B 117 (2013) 12953–12965.
[17] C. Che, Metal complexes of chiral binaphthyl schiff-base ligands and their application in stereoselective organic transformations, Coord. Chem. Rev. 242 (2003) 97–113.
[18] W.-S. Huang, Q.-S. Hu, L. Pu, From highly enantioselective monomeric catalysts to highly enantioselective polymeric catalysts: application of rigid and sterically regular chiral binaphthyl polymers to the asymmetric synthesis of chiral secondary alcohols, J. Org. Chem. 64 (1999) 7940–7956.
[19] Š. Vyskocil, M. Smrcina, V. Hanuš, M. Polášek, P. Kocovský, Derivatives of 2-amino-2'-diphenylphosphino-1,1'-binaphthyl (map) and their application in asymmetric palladium(0)-catalyzed allylic substitution, J. Org. Chem. 63 (1998) 7738–7748.
[20] D.-C. Jeong, H. Lee, K.S. Yang, C. Song, Effects of substituent on binaphthyl hinge-containing conductive polymers, Macromolecules 45 (2012) 9571–9578.
[21] S. Kang, I. Cha, J.G. Han, C. Song, Electroactive polymer sensors for chiral amines based on optically active 1,1′-binaphthyls, Mater. Express 3 (2013) 119–126.
[22] K. Akazaki, F. Toshimitsu, H. Ozawa, T. Fujigaya, N. Nakashima, Recognition and one-pot extraction of right- and left-handed semiconducting single-walled carbon nanotube enantiomers using fluorene-binaphthol chiral copolymers, J. Am. Chem. Soc. 134 (2012) 12700–12707.
[23] P. Deria, C.D. Von Bargen, J.-H. Olivier, A.S. Kumbhar, J.G. Saven, M.J. Therien, Single-handed helical wrapping of single-walled carbon nanotubes by chiral, ionic, semiconducting polymers, J. Am. Chem. Soc. 135 (2013) 16220–16234.
[24] D.-C. Jeong, H. Lee, K.S. Yang, C. Song, Effects of substituent on binaphthyl hinge-containing conductive polymers, Macromolecules 45 (2012) 9571–9578.
[25] J. Linshoeft, A.C.J. Heinrich, S.A.W. Segler, P.J. Gates, A. Staubitz, Chemoselective cross-coupling reactions with differentiation between two nucleophilic sites on a single aromatic substrate, Org. Lett. 14 (2012) 5644–5647.
[26] A.F.M. Kilbinger, W.J. Feast, Solution processable alternating oligothiophene-peo-block-co-polymers: synthesis and evidence for solvent dependent aggregation, J. Mater. Chem. 10 (2000) 1777–1784.
[27] J. Wang, R.M. Wolf, J.W. Caldwell, P.A. Kollman, D.A. Case, Development and testing of a general amber force field, J. Comput. Chem. 25 (2004) 1157–1174.
[28] J. Wang, P. Cieplak, P.A. Kollman, How well does a restrained electrostatic potential (RESP) model perform in calculating conformational energies of organic and biological molecules? J. Comput. Chem. 21 (2000) 1049–1074.
[29] D.A. Case, V. Babin, J.T. Berryman, R.M. Betz, Q. Cai, D.S. Cerutti, T.E. Cheatham III, T.A. Darden, R.E. Duke, H. Gohlke, et al., AMBER 14, University of California, San Francisco, CA, 2014.
[30] J.T. Frey, D.J. Doren, TubeGen 3.4, University of Delaware, Newark DE, 2011.
[31] A.W. Sousa da Silva, W.F. Vranken, ACPYPE - AnteChamber PYthon Parser interfacE, BMC Res. Notes 5 (2012) 367.
[32] M.J. Abraham, T. Murtola, R. Schulz, S. Páll, J.C. Smith, B. Hess, E. Lindahl, GROMACS: high performance molecular simulations through multi-level parallelism from laptops to supercomputers, SoftwareX 1–2 (2015) 19–25.
[33] B. Hess, H. Bekker, H.J.C. Berendsen, J.G.E.M. Fraaije, LINCS: a linear constraint solver for molecular simulations, J. Comput. Chem. 18 (1997) 1463–1472.
[34] W. Humphrey, A. Dalke, K. Schulten, VMD: visual molecular dynamics, J. Mol. Graph 14 (1996) 33–38.
[35] R.B. Weisman, S.M. Bachilo, Dependence of optical transition energies on structure for single-walled carbon nanotubes in aqueous suspension: an empirical kataura plot, Nano Lett. 3 (2003) 1235–1238.
[36] S.M. Bachilo, M.S. Strano, C. Kittrell, R.H. Hauge, R.E. Smalley, R.B. Weisman, Structure-assigned optical spectra of single-walled carbon nanotubes, Science 298 (2002) 2361–2366.
[37] S. Kazaoui, S. Cook, N. Izard, Y. Murakami, S. Maruyama, N. Minami, Photocurrent quantum yield of semiconducting carbon nanotubes: dependence on excitation energy and excition binding energy, J. Phys. Chem. C 118 (2014) 18059–18063.
[38] Y.K. Kang, O.-S. Lee, P. Deria, S.H. Kim, T.-H. Park, D.A. Bonnell, J.G. Saven, M.J. Therien, Helical wrapping of single-walled carbon nanotubes by water soluble poly(p-phenyleneethynylene), Nano Lett. 9 (2009) 1414–1418.
[39] J. Gao, M.A. Loi, E.J.F. de Carvalho, M.C. dos Santos, Selective wrapping and supramolecular structures of polyfluorene–carbon nanotube hybrids, ACS Nano 5 (2011) 3993–3999.
[40] H. Yang, V. Bezugly, J. Kunstmann, A. Filoramo, G. Cuniberti, Diameter-selective dispersion of carbon nanotubes via polymers: a competition between adsorption and bundling, ACS Nano 9 (2015) 9012–9019.
[41] J. Wang, R.M. Wolf, J.W. Caldwell, P.A. Kollman, D.A. Case, Development and testing of a general amber force field, J. Comput. Chem. 25 (2004) 1157–1174.
[42] J. Wang, P. Cieplak, P.A. Kollman, How well does a restrained electrostatic potential (RESP) model perform in calculating conformational energies of organic and biological molecules? J. Comput. Chem. 21 (2000) 1049–1074.